THE PENNSYLVANIA STATE UNIVERSITY
SCHREYER HONORS COLLEGE

DEPARTMENT OF AEROSPACE ENGINEERING

LONGITUDINAL CONTROL VIA DISTRIBUTED PROPULSION AND ELEVATOR DEFLECTION

CHARLOTTE GILL
SPRING 2014

A thesis
submitted in partial fulfillment
of the requirements
for a baccalaureate degree
in Aerospace Engineering
with honors in Aerospace Engineering

Reviewed and approved* by the following:

Jack W. Langelaan
Associate Professor of Aerospace Engineering
Thesis Supervisor

Philip J. Morris
Boeing A.D. Welliver Professor of Aerospace Engineering
Honors Adviser

George A. Lesieutre
Professor of Aerospace Engineering
Head of Aerospace Engineering

* Signatures are on file in the Schreyer Honors College.

ABSTRACT

An aircraft can be controlled without the use of control surfaces by applying differential thrust across multiple motors. Trimming the aircraft without elevator has the potential to reduce the trim drag during cruise, which would improve the aircraft's flight efficiency. Differential thrust was analyzed for a SB-XC (a 14 foot wingspan RC aircraft) at trim conditions by modeling the aircraft using linearized longitudinal equations of motion. Longitudinal flight control is examined using a combination of differential thrust to trim the aircraft and elevator deflection for disturbance rejection. The configuration of the motors for longitudinal control is analyzed by varying the static margin and C_{m0} of the aircraft to compute the necessary moments from the thrust force for the aircraft to trim across a wide range of flight conditions. Longitudinal control is implemented using successive loop closure: elevator controls pitch angle and pitch angle is used to control airspeed. The total thrust controls the climb rate, so trim is achieved by calculating the difference in thrust that results in zero pitching moment at the desired flight condition. A flight speed controller and rate of climb controller were designed using the root locus method to optimize the aircraft response. From this model it was found that it is possible to use differential thrust to trim an aircraft at different commanded speeds and rates of climb while using the elevator to correct for small disturbances.

TABLE OF CONTENTS

LIST OF FIGURES

ACKNOWLEDGEMENTS

I would like to thank my thesis advisor, Dr. Langelaan, for helping me learn more about simulating aircraft dynamics and modeling aircraft controls. I really appreciate the amount of time he has spent to help answer my questions and point me in the right direction as I conducted this study. I would also like to thank the professors in the aerospace engineering department for providing me with the knowledge necessary to write a thesis on my topic.

Chapter 1

Introduction

The distributed propulsion analysis was conducted on a SB-XC, a 14-foot wingspan RC aircraft pictured in Fig. 1. Dr. Jack Langelaan's Air Vehicle Intelligence and Autonomy laboratory currently possesses two of these aircraft. They are used for dynamic soaring research and therefore the parameters for the vehicle have been previously calculated and are found in Appendix A[1].

Figure 1: A Graduate Student Holding the SB-XC

Besides the vehicle properties being known, this aircraft also has the capability to be powered by electric propulsion. Depending on the response times of the motors, differential thrust could serve as the primary longitudinal control for smaller aircraft. Electric propulsion allows for quick motor responses and therefore distributed propulsion for control of the aircraft.

A study was conducted by NASA[2] using an engine dynamic model based on actual flight test data, and it was found that the engine delay is larger at lower velocities and less at higher velocities and certain altitudes. Too large of a delay would increase the difficulty of controlling the aircraft. Therefore differential thrust at higher speed flight could provide an adequate amount of response time for consideration as a means of aircraft control.

The use of distributed propulsion as opposed to elevator deflection for trimming has the potential to increase aircraft efficiency by reducing trim drag during flight[3]. A down force from the tail is necessary to balance out the nose down moment caused by the lift from the wing. This down force results in an increase in necessary lift for steady level flight, increasing drag. However, because differential thrust would provide the necessary moments for trimming the aircraft, elevator deflection is not required and no additional drag forces occur. Due to the delay in response, distributed propulsion among the motors could be used for damping out longer periods of oscillations, such as the phugoid mode, while the elevator is used to correct for the small disturbances so the aircraft is able to maintain trimmed flight. Therefore the SB-XC was modeled with no flaps and the trim elevator is set to zero to allow for the thrust differential to trim the aircraft at different commanded velocities.

Differential thrust also has applications for larger aircraft. When an aircraft loses power to the hydraulic systems that move its flight controls, another means of control must be readily available. This type of failure has happened previously, with some pilots able to regain control and some unable to do so. On July 19, 1989, United Airlines Flight 232, a DC-10, lost power to its systems when a tail-mounted engine experienced catastrophic failure during flight and damaged the hydraulic lines. With no control surfaces, the pilots managed to land the aircraft by using differential thrust. This landing resulted in casualties due to the lack of complete control by

using just the engine thrust, and the speed at which they were forced to land without the use of flaps[4]. Another case was when an A300-B4 was taking off from Baghdad and was struck by a missile, causing it to lose all hydraulic systems and some of the surface of the left wing. The pilots quickly had to learn how to use the engines for pitch and roll control, and managed to land the aircraft safely. During the flight, they realized that they could control the aircraft's pitch with thrust, but had to give up control over speed. Lateral control was also possible, but the response was slower than when using control surfaces[5]. Exploring differential thrust of engines provides another means of aircraft control in the event of an emergency.

The use of the motors for differential thrust depends on their location with respect to the aircraft's center of gravity (c.g.). If the motors are located below the c.g., they will cause a nose up pitching moment, and if they are above they will cause a nose down pitching moment. The larger the distance from the thrust line to the aircraft's c.g., the greater the moments from the motor and smaller the difference in thrust has to be. This results in the aircraft's speed becoming dependent on the pitch and change in thrust. Increasing the thrust of the aircraft initially increases its speed, which creates an upward pitching moment. In order to design a controller for an aircraft to use differential thrust to fly at trim at different velocities without pitching and climbing or descending, the flight altitude must also be held constant.

Before the controllers could be modeled in Simulink[6], the architecture first needed to be designed. The two inputs for the model are flight speed and rate of climb or descent. Flight speed is controlled by pitch angle, which is controlled by elevator deflection. The rate of climb is controlled by the thrust from the motors. This elevator deflection and thrust force go into the aircraft dynamics block to be used along with other aircraft parameters to find C_L, C_D, and C_M. These coefficients are used in solving for the forces and moments experienced by the SB-XC,

which are then used in the longitudinal equations of motion. Once these equations are solved, they can be integrated and fed back into the aircraft dynamics block to be used to find the solution for the next time step.

A block diagram of the Simulink model can be seen in Fig. 2. In this model, a velocity is commanded and the error between the desired velocity and actual velocity, which is calculated using the aircraft dynamic equations, is computed. This error then goes into a controller that outputs a commanded pitch angle. The actual aircraft pitch angle, which is calculated in the aircraft dynamics block, is then subtracted from this required pitch angle to result in the pitch error, which then goes into the controller that drives the elevator deflection. This deflection angle then gets added to the trim elevator value to produce the necessary elevator deflection to correct for the error in pitch angle and velocity. The error between the commanded rate of climb and actual rate of climb is calculated in the rate of climb loop and goes into a controller that computes the necessary power. The power is divided by velocity to obtain thrust, and then added to the trim thrust for a certain flight condition to calculate the total thrust necessary to achieve the desired rate of climb. In order to find the thrust difference from trim, an equation for the pitching moment was derived to account for asymmetric propulsion. The total thrust and thrust difference are used to calculate the forces needed from each motor, and these values go into the aircraft dynamics block to compute the aircraft forces and moments.

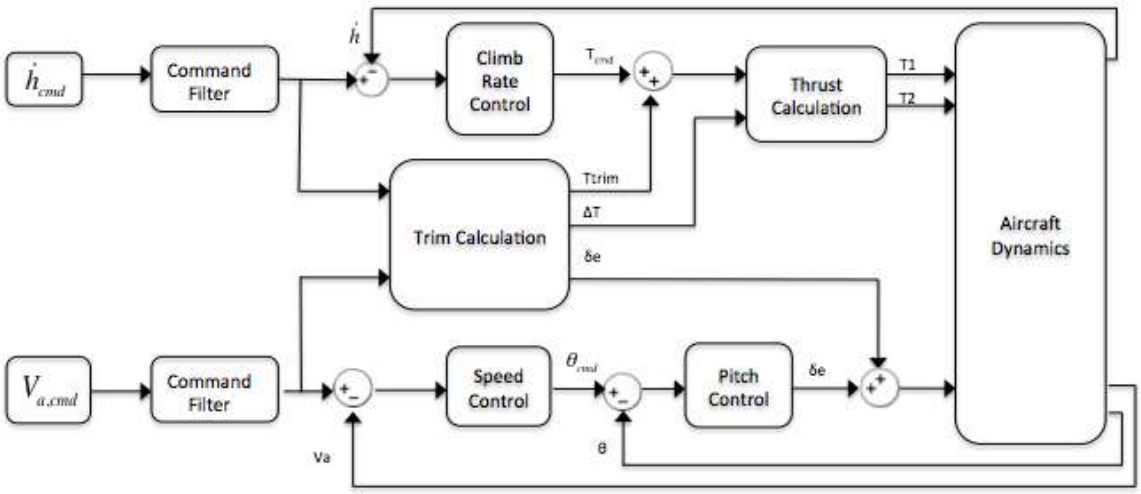

Figure 2: A High Level Diagram of the Simulink Model

Chapter 2

Pitch Dynamics and Trim Calculations

Longitudinal Equations of Motion

Flight parameters for the SB-XC needed to be calculated to find an ideal trim condition for distributed propulsion across the upper and lower motors. This required placing the motors at a reasonable distance, z, away from the c.g. to allow for a large enough moment from the thrusts yet at the same time also not be in the way of landing. In this longitudinal analysis, the top and bottom motors are referred to as motor 1 and motor 2 respectively, as seen in Fig. 3.

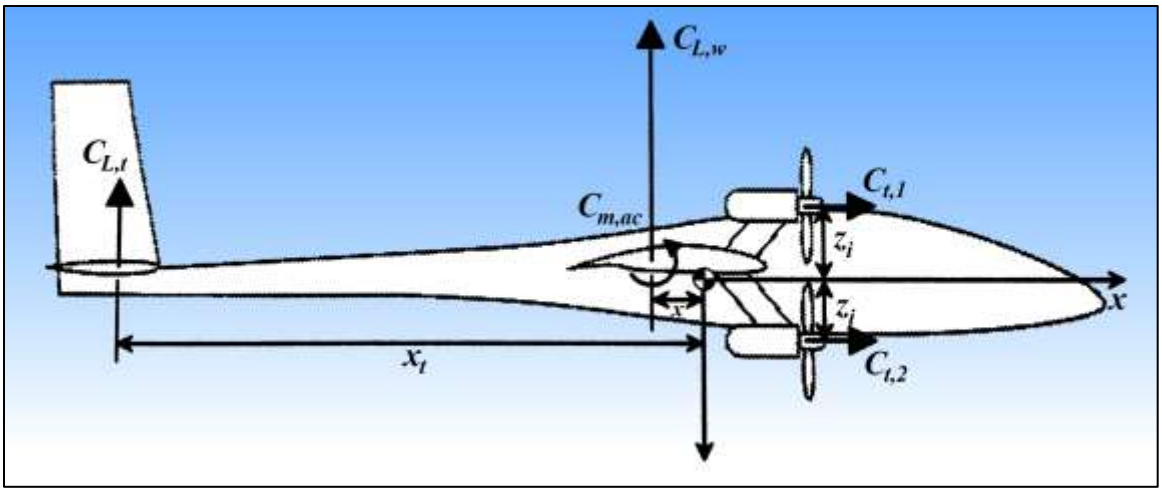

Figure 3: A Diagram of the SB-XC

In order to model the dynamic response of the aircraft, the longitudinal equations of motion were linearized to take into account the elevator deflection and thrust forces from the motors. Linearizing the equations of motion decouples the longitudinal dynamics from the lateral dynamics, allowing the differential thrust analysis to focus solely on this type of motion. For this

approximation, the lateral states (roll, yaw and the velocity in the y direction) were assumed to be zero. The linearized equations are used to calculate the longitudinal states $\dot{x}$, $\dot{z}$, $\dot{\theta}$, $\dot{q}$, $\dot{u}$, and $\dot{w}$. These dynamic equations are then integrated to find the aircraft states that are used as the flight conditions for the calculations at the next time step. The state equations are found in Etkin[7] and are:

$$\dot{u} = \frac{\frac{1}{2}\rho v^2 S(C_L\alpha - C_D + C_{T1} + C_{T2})}{m} - gsin\theta - qw \tag{1}$$

$$\dot{w} = \frac{\frac{1}{2}\rho v^2 S(-C_D\alpha - C_L)}{m} + gcos\theta + qu \tag{2}$$

$$\dot{q} = \frac{\frac{1}{2}\rho v^2 ScC_M}{I_{yy}} \tag{3}$$

$$\dot{\theta} = q \tag{4}$$

$$\dot{x} = ucos\theta + wsin\theta \tag{5}$$

$$\dot{z} = -usin\theta + wcos\theta \tag{6}$$

The equations used to calculate the lift the drag coefficients are :

$$C_L = \frac{c}{2v} + C_{Lq}\dot{\theta} + C_{L0} + C_{L\alpha}\alpha + C_{L\delta e}\delta e \tag{7}$$

$$C_D = 0.1723\varphi^4 - 0.3161\varphi^3 + 0.2397\varphi^2 - 0.0624\varphi\_0.0194 \tag{8}$$

where,

$$\varphi = C_{L0} + C_{L\alpha}\alpha \tag{9}$$

Controlling the pitch and rate of climb of the aircraft requires analysis of the pitch dynamic equations, which are Eqs. (3) and (4). The pitch rate is determined by calculating the parameters that affect the aircraft's moment coefficient and then rewriting Eq. (3) as

$$\dot{q} = \ddot{\theta} = \frac{(1/2)\rho v^2 Sc}{I_{yy}}[C_{m0} + C_{m\alpha}\alpha + C_{mu}u + C_{mq}q + C_{m\dot{\alpha}}\dot{\alpha} + C_{m\delta e}\delta e + \left(\frac{z}{c}\right)(C_{T2} - C_{T1})] \tag{10}$$

Eq. (10) shows that by trimming the aircraft with zero elevator deflection, a difference in the thrust coefficients can be utilized as needed to result in a change of pitching rate of zero. It can also be seen how the change in thrust will change the aircraft's pitch angle, and therefore velocity.

Aircraft Parameters for Trim

Most of the aircraft properties were found previously and are used for the calculations performed for the flight speed and rate of climb controller design. In order to use thrust to trim the aircraft instead of the elevator, ideal locations for the motors must be found to create a large enough moment arm so the thrust forces are able to adequately control the longitudinal motion of the aircraft. The moment equation can be rewritten to include thrust, so

$$C_m = C_{m0} + C_{m\alpha}\alpha + C_{m\delta e}\delta e - C_{T1}\left({}^{z}/_{c}\right) + C_{T2}\left({}^{z}/_{c}\right) \tag{11}$$

During trimmed flight, the thrust force must equal the drag force on the airplane, hence

$$C_D = C_{T1} + C_{T2} \tag{12}$$

Solving Eqs. (11) and (12) for $C_{T1}$and C_{T2} and setting the elevator deflection to zero for steady level flight allows these thrust coefficients to be plotted over a range of motor locations for the given aircraft trim properties. Fig. 4 shows that having a C_{m0} of zero and a high static margin does not allow both thrusts to be positive. No matter what the value of z is, the parameters of the SB-XC resulted in the difference between the necessary thrust outputs from both motors becoming larger than the total thrust needed for the airplane to fly at trim, or larger than the aircraft's drag. Having the difference be so large results in one of the thrust forces being negative, which is undesirable.

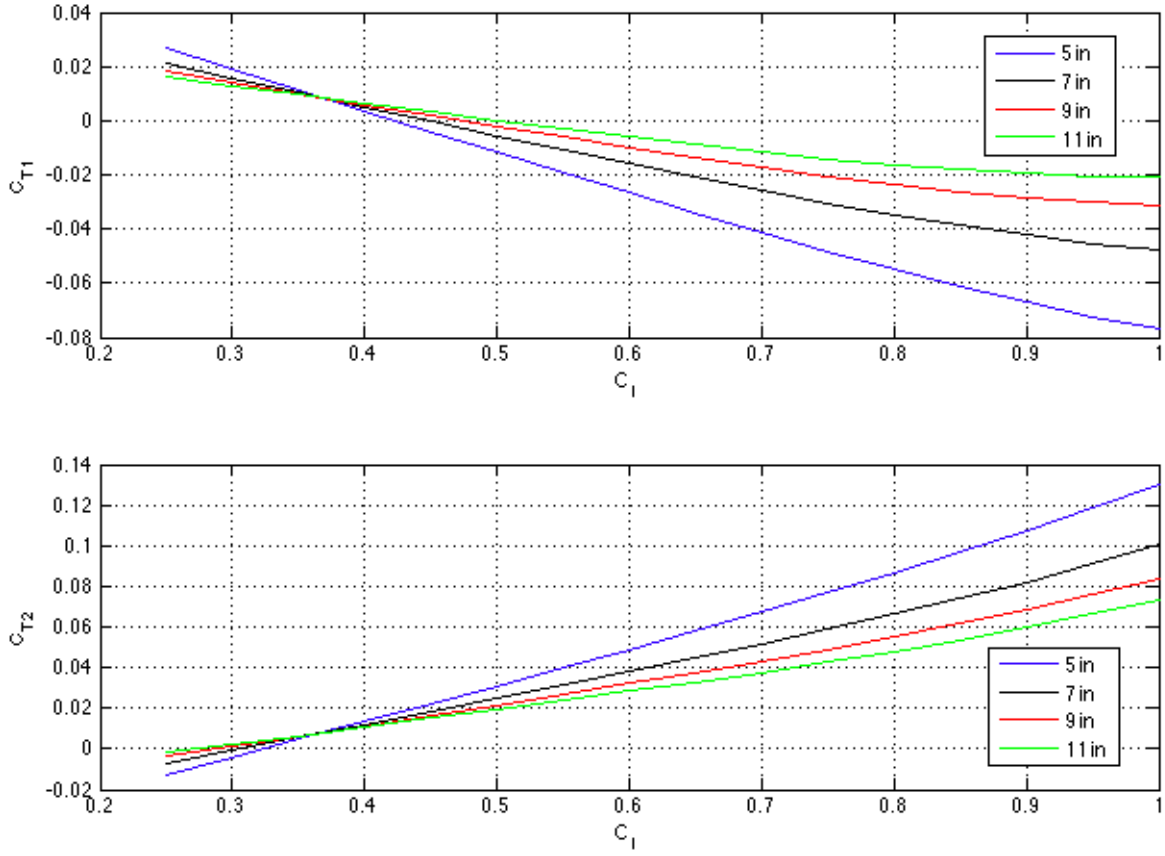

Figure 4: C_T vs. C_l Before C_{m0} and Static Margin Calculations

In order to find values for z that would not result in a negative thrust coefficient, C_{mo} and the static margin were varied. The static margin, K_n, affects the stability and controllability of an aircraft. Since it is equal to the distance from the location of the center of gravity and the neutral point of the aircraft, this parameter can be changed by moving the c.g. forward or aft as needed. Changing the static margin affects the moment since

$$C_{m\alpha} = C_{L\alpha} K_n \tag{13}$$

Since the value of $C_{m\alpha}$ must be negative for the aircraft to be stable, Eq. (13) shows that the static margin must remain a negative value because $C_{L\alpha}$ is positive. By making K_n less negative, the aircraft is becoming less statically stable and easier to control with the differential

thrust. Eq. (11) and Eq. (12) are re-written as C_{T1} and C_{T2} in terms of the static margin K_n, by substituting Eq. (13) for $C_{m\alpha}$, and become

$$C_{T1} = \left(\frac{-c}{2z}\right)(-C_{m0} + C_{L\alpha}K_n\alpha) + \frac{1}{2}C_D \quad (14)$$

$$C_{T2} = \left(\frac{-c}{2z}\right)(C_{m0} - C_{L\alpha}K_n\alpha) + \frac{1}{2}C_D \quad (15)$$

The affect of static margin and C_{m0} can be analyzed by plotting the thrust coefficients as a function of static margin while varying C_{m0}. In order to have these two be variables, the flight condition was chosen to be trim flight; the velocity is 15.5 m/s, the angle of attack is 1°, the C_L is 0.67. The motor location was selected to be 9.5 inches from the c.g. The plot in Fig. 5 shows how the difference in thrust is affected by an increase in C_{m0} and decrease in the static margin. Since the thrust difference must be smaller than C_D for both motors to have a positive thrust, the drag coefficient was also plotted as a purple horizontal constant line to show where the difference is too large.

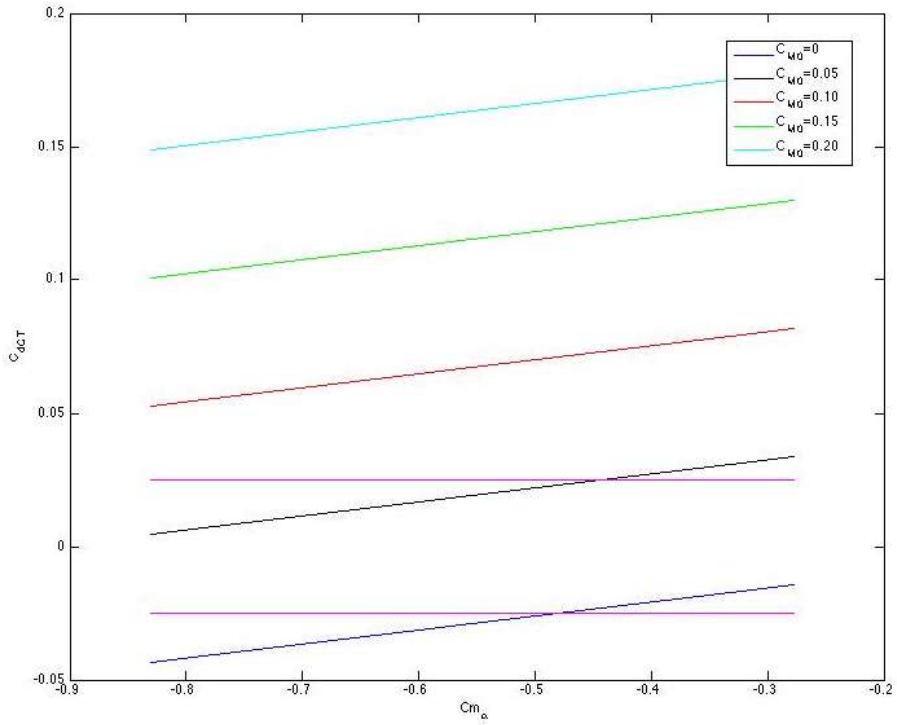

Figure 5: Affect of C_{m0} and the Static Margin on the Thrust Difference

As shown in Fig. 5, an increase in C_{m0} results in a larger thrust difference, or more negative C_{T2} and more positive C_{T1}. This is because increasing the pitching moment requires the difference in thrusts to also increase. However, since they both must still equal the force from drag, one must become more negative to allow for the larger dC_T. Since this is the issue that is trying to be resolved, C_{m0} is kept at a small value between 0 and 0.05 to keep dC_T small and both thrust values positive. Fig. 5 also shows that the ideal static margin is between 10-15%.

The other parameter that affects the values of C_{T1} and C_{T2} is C_{m0}. Since $C_{m\alpha}$ is picked to be a negative value for stability, a positive value of C_{m0} is chosen to make the aircraft trimmable. An increase in C_{m0} results in a more negative C_{T2} and more positive C_{T1}, or a greater dC_T. This is because increasing the pitching moment requires the difference in thrusts to also increase. However, since they both must still equal the force from drag, one must become more negative

to allow for the larger dC_T. Since this is the issue that is trying to be resolved, C_{m0} is kept at a small value to keep dC_T small and both thrust values positive.

By varying C_{m0} and K_n for a range of motor configurations, a good set of values were found to be 0.01 for C_{m0}, 5% for K_n, and 9.5 inches for z. As shown in Fig. 6, this motor location allows for a positive thrust over a wide range of C_l values, yet does not interfere with takeoff and landing. The distance from the motors to the c.g. must take into account the height of the wing from the ground so that ground clearance is still easily managed.

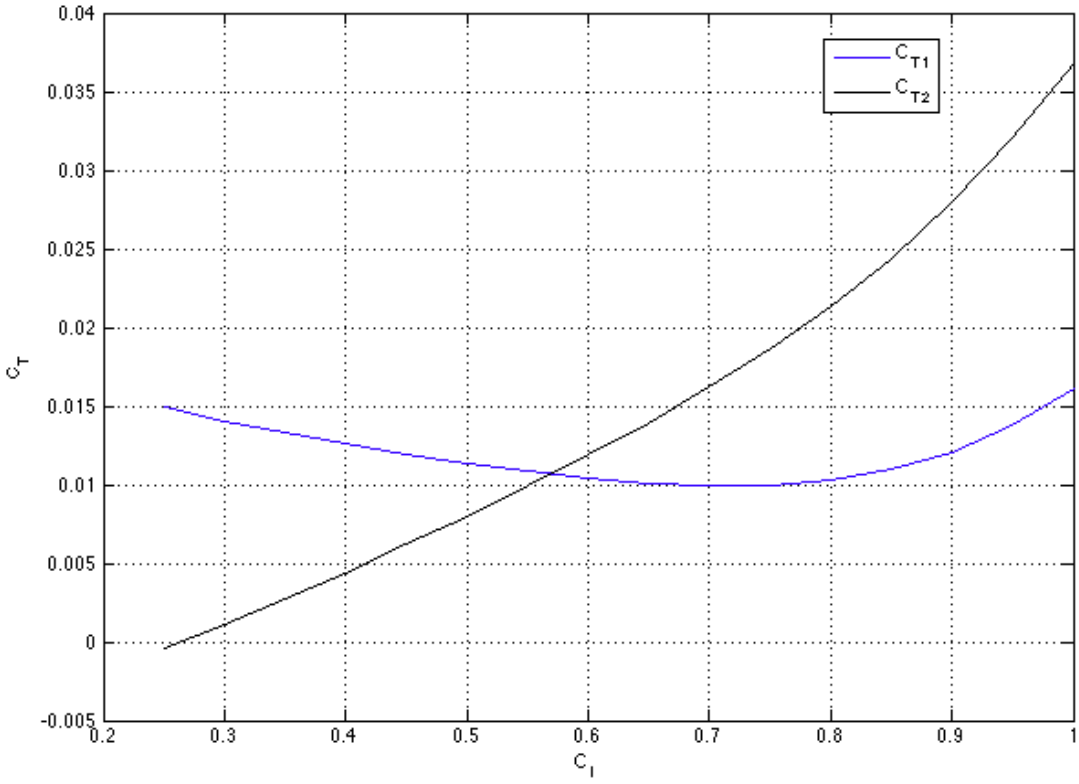

Figure 6: C_T vs. C_l After Calculating Ideal C_{m0} and Static Margin

Chapter 3

Flight Control

Pitch Angle and Airspeed Controller

The first step to modeling the longitudinal motion of the SB-XC was to design the flight speed controller using MATLAB[8] and Simulink. Before the model can be created in Simulink, the control loop architecture has to be designed. The model will input a commanded velocity, which will be controlled by the aircraft's pitch angle. As learned by the pilots of the A-300 that lost power to its hydraulics due to a missile strike, the thrust from the motors allows the pilot to control the pitch angle of the aircraft, which subsequently affects the speed. An increase in pitch angle will cause an increase in lift, which ultimately leads to a decrease in velocity and altitude. Besides thrust, another way to control the pitch angle of the aircraft is by deflecting the elevator. A positive elevator deflection (trailing edge down) results in a nose-down pitching moment and a negative deflection results in a nose-up moment. Since the bandwidth of a motor is typically lower than that of a control surface, the elevator is used for the higher frequency dynamics, such as the short period mode. Once these relationships were established, this loop was modeled in Simulink.

In Fig. 2, a block diagram of the Simulink model, a velocity is commanded and the error between the desired velocity and actual velocity, which is calculated using the aircraft dynamic equations, is computed. This error then goes into a controller that outputs a commanded pitch angle. The actual aircraft pitch angle, which was calculated in the aircraft dynamics block, is then fed back into the system to obtain the pitch error, which then goes into the controller that

drives the elevator deflection. This deflection angle then gets added to the trim elevator value to produce the necessary elevator deflection to correct for the error in pitch angle and velocity.

In order for the system to behave as required, the root locus method can be used to place desired close loop poles and zeros for the controller design. After finding the transfer functions for the system, the sisotool function in MATLAB can be used to find the ideal pole and zero locations. These locations create a compensator, which can then be used to find the value of K_p, K_i, and K_d as necessary. Besides using sisotool, these values can also be calculated by hand for a designated rise time and damping ratio. Once these values are found, the controller can be added to the model, and tuned as required using the PID tuner in Simulink. This allows the response times to be changed to provide the desired speed of the loop.

Pitch Angle to Elevator Deflection

The first loop to be designed was the inner loop that relates pitch angle to elevator deflection. This loop will have the fastest response time so that the elevator can be adjusted to deal with disturbance rejection. Taking the derivative of the change in pitch rate,$\dot{q}$, and assuming small angle approximation so that α=θ, Eq (10) can be rewritten as

$$\ddot{\theta} = \frac{(1/2)\rho v^2 Sc}{I_{yy}}[C_{m0} + C_{m\alpha}\theta + C_{mu}u + C_{mq}\dot{\theta} + C_{m\dot{\alpha}}\dot{\theta} + C_{m\delta e}\delta e] \qquad (16)$$

In order to design a controller for this loop, Eq. (14) is used to find the relationship between the change in pitch angle and the elevator deflection. Taking the Laplace transform of Eq. (16) results in the transfer function relating the two values to be

$$\frac{\Theta(s)}{\delta e(s)} = \frac{C_{m\delta e}}{s^2 - s(C_{mq} + C_{m\dot{\alpha}}) - C_{m\alpha}} \qquad (17)$$

Because the response time for the loop needs to be quick, with a settling time of around one second, the equation for the settling time, which is found in Franklin[9], can used to solve for the natural frequency, ω_n, using a damping ratio, ζ, of one so that the system is critically damped. This equation is

$$t_s = \frac{4.6}{\zeta \omega_n} \tag{18}$$

Once the natural frequency is found, the PID gains can be calculated. By multiplying the equation for a PID controller,

$$K(s) = \frac{K_d s^2 + K_p s + K_i}{s} \tag{19}$$

by Eq. (15), the desired response can be achieved. The characteristic equation of this result can be found and left in terms of the proportional gain, K_p, the integral gain, K_i, and the derivative gain, K_d. In order to solve for these variables, another characteristic equation must be written in which a 3rd pole, σ_3, is chosen so as to have a little effect on the system and is written as

$$(s - \sigma_3)(s^2 + 2\zeta\omega_n s + \omega_n^2) \tag{20}$$

This third pole can be set to equal $-4\sigma_1$, where σ_1 is equal to the damping ratio times the natural frequency found by solving Eq. (18). Setting Eq. (20) equal to the characteristic equation with the gains as variables allows the values of the gains to be found. From this method, initial gain values were found of K_i= -13.178, K_p= -6.4114, and K_d= -0.44.

These gains were used to create a PID controller in Simulink. After the controller was added to the model, they were tuned using the PID tuner. Using this allows the gains to be adjusted as necessary to change the settling time or overshoot of the controller. The final result is seen in the closed loop step response plot in Fig. 7. A controller the a transfer function of

$$G(s) = \frac{-0.482s^2 - 2.991s - 3.526}{s} \tag{21}$$

results in a settling time 0.939 seconds and an overshoot of 6.51%.

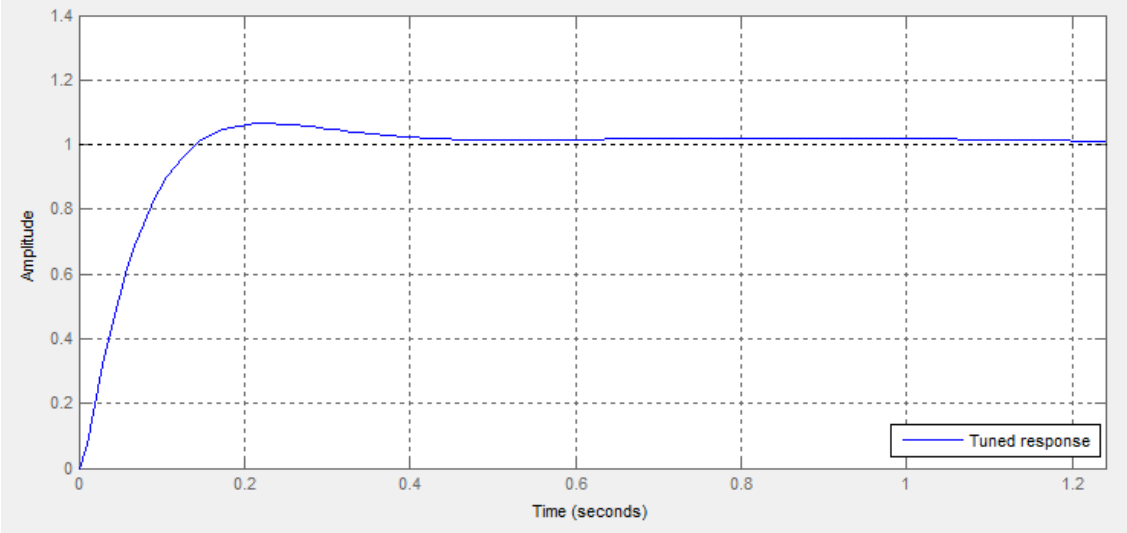

Figure 7: Closed Loop Step Response of $\frac{\Theta(s)}{\delta e(s)}$

Velocity to Pitch Angle

Velocity Input

The velocity input is a step function that has an initial condition of the trim velocity value of the aircraft and a final value of the desired velocity value. The step time is one second. Because the motor response is not instantaneous, the velocity cannot be input as a step function that changes velocity values instantaneously. Therefore, a filter must be added to this input to smooth out the velocity step function. This filter is written as

$$\frac{V^*}{V_{cmd}} = \frac{\omega_n^2}{s^2+2\zeta\omega_n s+\omega_n^2} \tag{22}$$

This transfer function has a damping ratio of one and rise time, t_r, that depends on the size of the change in velocity for a smoother curve. For a difference of less than 2 m/s, t_r=2, if

the difference is between 2 m/s and 4 m/s, t_r=3, and above 4 m/s t_r=4. This rise time is then used to calculate the natural frequency using Eq. (18).

Using this ω_n value, Eq. (22) can then be converted to state space form. The reason for this is that the transfer function blocks in Simulink do not allow for an initial condition to be added, while a state space block can. The two equations used to calculate the matrices for the state space function are found in Franklin[8] and are

$$\dot{x} = Ax + Bu \qquad A = \begin{bmatrix} -2\zeta\omega_n & -\omega_n^2 \\ 1 & 0 \end{bmatrix} \qquad B = \begin{bmatrix} 1 \\ 0 \end{bmatrix} \tag{23}$$

$$y = Cx + Du \qquad C = [0 \quad \omega_n^2] \qquad D = [0] \tag{24}$$

$$Inital\ condition = \begin{bmatrix} 0 & \frac{V_{trim}}{\omega_n^2} \end{bmatrix} \tag{25}$$

The Controller

Once the inner loop controller for the pitch angle to elevator deflection relation was created, the outer loop could be designed. Like the previous controller, the first step for this one was to find the transfer function that relates the aircraft's airspeed to its pitch angle. This was found by rewriting the force equation of the aircraft. The forces in the x-direction of the aircraft are thrust, drag, and a component of lift, which is dependent on the pitch angle of the aircraft. These forces can be written as

$$ma = m\dot{v} = T - D - mgsin\theta \tag{26}$$

Since in steady level flight thrust equals drag, Eq. (26) can be simplified in terms of the airspeed of the aircraft and its pitch angle. The Laplace transform can then be taken of this simplified equation and the transfer function is found to be

$$\frac{V_a(s)}{\Theta(s)} = \frac{-g}{s} \quad (27)$$

The root locus plot of the transfer function shows that a negative proportional gain is needed to place the roots of the transfer function in the left hand plane of the graph. Any roots in the right hand plane could cause the system to go unstable. Using the root locus method and sisotool, the value for the proportional gain can be calculated and the root locus plot can be seen in Fig. 8. Because the inner loop of pitch angle to elevator deflection was designed to have a settling time of 0.939 seconds, the outer loop will be designed to have a setting time of around 3 seconds in order to allow the inner loop time to run inside the outer loop. The compensator was found to be -0.1334 by placing the gain at -1.31 on the real axis.

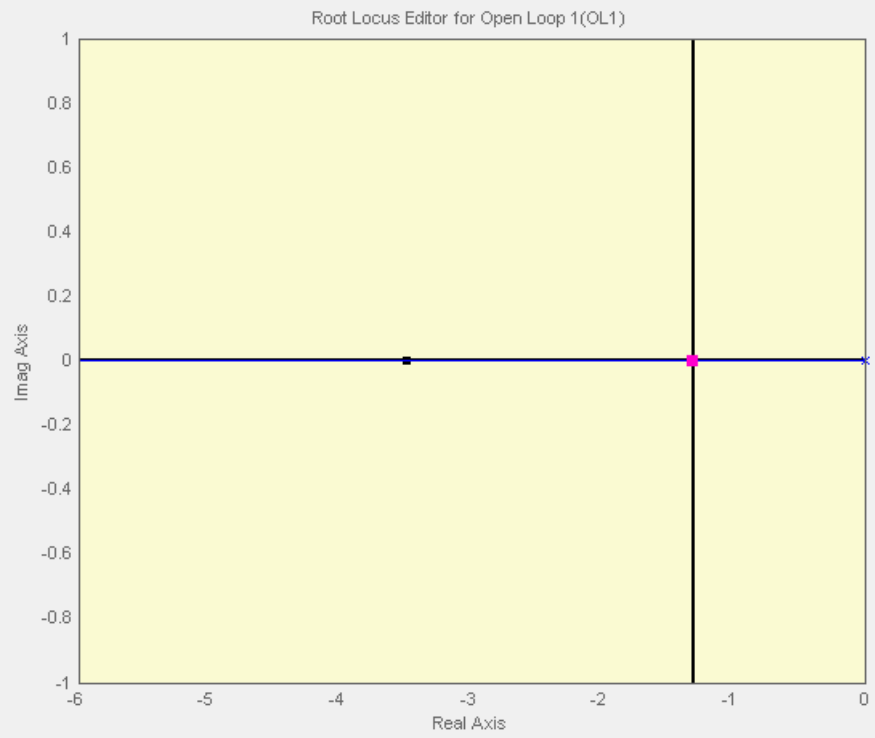

Figure 8: Root Locus of $\frac{V_a(s)}{\Theta(s)}$

Using the PID tuner in Simulink, the value for the controller parameters can be tuned for the desired response by plotting the closed loop step response, shown in Fig. 9. A proportional gain of -0.244 provided a settling time of 3.34 seconds with an overshoot of 34%. The transfer function for this controller is therefore

$$G(s) = -0.244 \tag{28}$$

Trying to decrease this overshoot with a proportional gain increased the settling time by a decent amount. Decreasing the overshoot by half resulted in a two times increase in settling time and five times increase in rise time, which results in too slow of a response.

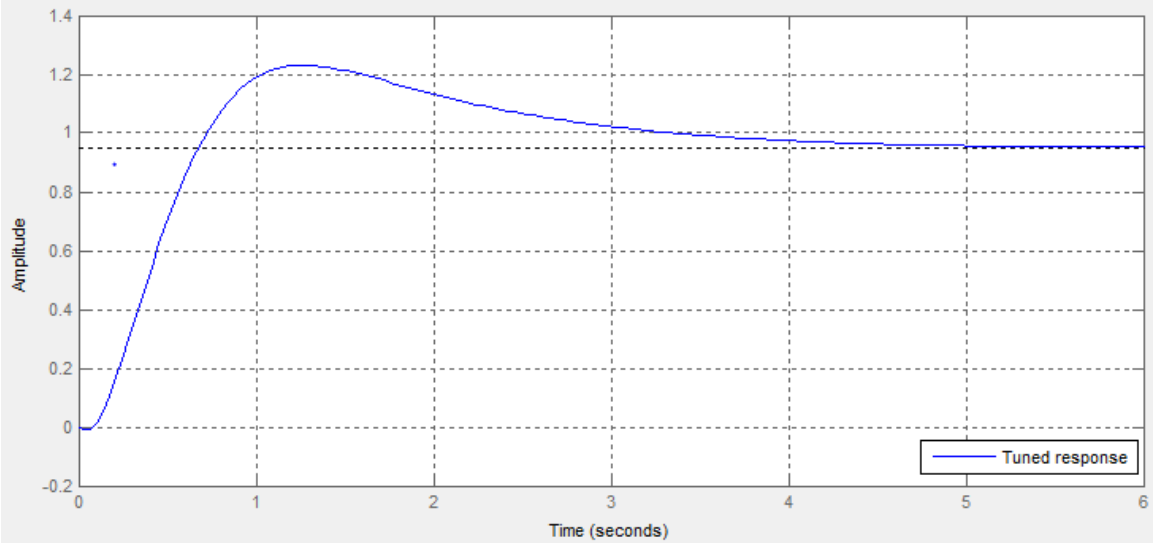

Figure 9: Closed Loop Step Response of $\frac{V_a(s)}{\Theta(s)}$

Rate of Climb Controller

The rate of climb of the aircraft will be controlled by the total thrust output from all the motors. The greater the difference between the power available, which is currently being commanded to the motors, and the power required for the aircraft to fly at a certain set of conditions, the larger the rate of climb will be. Once the total thrust necessary for the specified

climb rate is calculated, a difference in thrust from the motors can be computed by summing the moments of the aircraft and finding the thrust outputs required to maintain either steady level flight or a steady climb or descent. This total thrust and thrust difference are then used to calculate the forces needed from each motor. Since the motors have a greater lag in response time than elevator deflection does, they will be used for trimming the aircraft and low frequency dynamics, such as the phugoid mode.

As with the other controllers, the first step to designing the controller for the rate of climb of the aircraft was finding the transfer function that relates rate of climb and thrust. An equation that is used to calculate the rate of climb of an aircraft, it can be rewritten in terms of the excess power of the aircraft since the thrust required must equal the drag of the SB-XC for trim:

$$\dot{h} = \frac{P_{avail} - P_{req}}{mg} = \left(\frac{T_{excess} + (T_{req} - D_{req})}{mg}\right) v \tag{29}$$

Taking the Laplace of Eq. (29) results in the transfer function relating the rate of climb to the thrust to be written as

$$\frac{J(s)}{P(s)} = \frac{1}{mg} \tag{30}$$

The root locus plot in Fig. 10 shows that an integral controller is necessary to place all the roots of the transfer function in the left hand plane of the graph. In MATLAB's sisotool toolbox, a settling time and damping ratio requirement can be plotted and used to find the location of the gain for the compensator. A desired settling time of nine seconds and a damping ratio of one were chosen. The settling time was chosen to take into account the lag from the motors. The response from the motors will not be as quick as the response from the elevator since it is only being used to keep the aircraft flying at trim and correcting for the phugoid mode. The gain can

then be placed where these two plotted requirements intersect, and was found to be located at -0.435 along the real axis, which gives a compensator with a pole at zero and gain of 42.6.

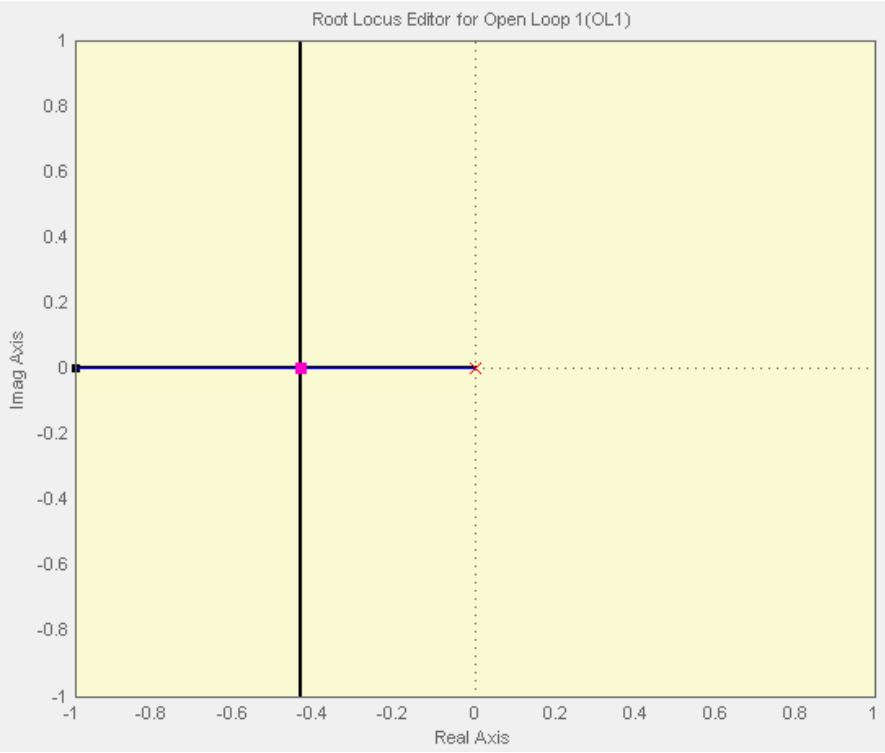

Figure 10: Root Locus of $\frac{J(s)}{P(s)}$

After creating the integral controller in the Simulink model, the PID tuner was used to tune the gains for the desired system response. The plotted close loop step response in Fig. 11 shows that the gain found from the root locus method resulted in an adequate response and the controller is therefore

$$G(s) = \frac{42.6}{s} \tag{31}$$

The rise time is 8.44 seconds and there is a 0% overshoot.

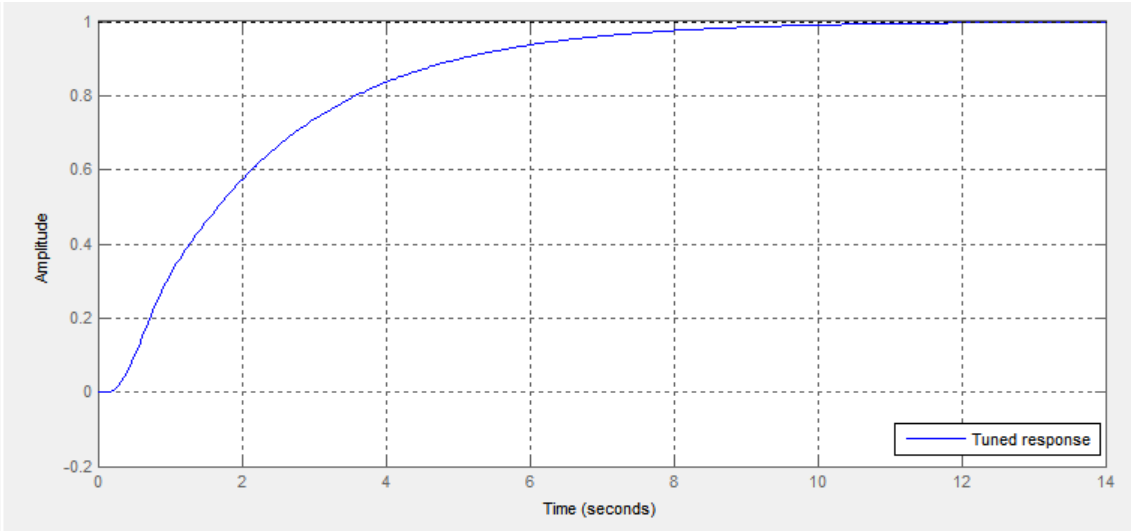

Figure 11: Closed Loop Step Response of $\frac{J(s)}{P(s)}$

Computing Desired Thrust

While designing the controller to control the rate of climb of the aircraft, a way of distributing the total thrust among the motors must also be found. Since the differential thrust is aiming to keep the SB-XC flying at trim, the sum of the moments of the aircraft must equal zero. Eq. (11) can be re-written as

$$C_{mdt} = C_{T1} - C_{T2} = \frac{c}{z}(C_{m0} + C_{m\alpha}\alpha) \tag{32}$$

by assuming the sum of the moments is zero for steady level flight and elevator deflection is not used to trim the aircraft. The difference between the thrust from the two motors is dependent on the angle of attack of the aircraft. This is reasonable since the thrusts will need to be able to trim the aircraft over a range of angle of attacks as the aircraft climbs or descends.

Since the total aircraft thrust must equal the drag for trimmed flight, the trim thrust required for a desired flight condition is added to the thrust value that is output from the controller. This total thrust then is used with the thrust difference to calculate the individual

forces needed from each motor. Knowing that T_{total} is the sum of the thrusts and C_{mdt} is the difference between the two thrust coefficients, two sets of equations can be written and solved in terms of T_1 and T_2 and are

$$T_1 = \frac{T_{total} + (1/2)\rho v^2 S C_{mdt}}{2} \quad (33)$$

$$T_2 = \frac{T_{total} - (1/2)\rho v^2 S C_{mdt}}{2} \quad (34)$$

These forces are used in calculating the forces and moments in the aircraft dynamic computations.

After running the model, it was found that some of the run cases resulted in negative thrust. Negative or reverse thrust is not desired for a couple of reasons. For one, reverse thrust adds drag since it acts in the direction opposite to the motion of the aircraft and therefore reduces aircraft efficiency during flight. In addition, many aircraft currently do not have the option to use reverse thrust during flight due to safety precautions. There have been incidents where reverse thrust was turned on during flight due to a mechanical problem, and resulted in the loss of the aircraft, such as the fatal Lauda 767 incident. The reverse thrust on the left engine of the Lauda 767 was deployed mid-flight, causing the aircraft to dive and break up mid-air[10].

When an aircraft needs to slow down or descend, drag needs to be added to slow the aircraft or descend it at a commanded rate, which can be done by deploying flaps or spoilers. Since the model does not have the capability to use flaps or spoilers, reverse thrust is needed in some cases. For some of the descent run cases, the total thrust required for the desired rate of descent is negative. This was allowed for the model since the aircraft needs the negative total thrust to respond as desired. For the cases where the total thrust was positive, but the difference

in thrust between the motors was greater than the total, reverse thrust was not allowed. Instead, the motor that had a negative thrust value was set to zero, and the other motor was set to equal the total thrust value necessary to keep the aircraft flying at the desired velocity. The elevator is then deflected to produce the necessary moment to trim the aircraft with the new thrust difference. When modeling the thrusts and changing their values in the event of a negative thrust force, the engine lag is not taken into account and an instantaneous change in thrust was assumed.

Chapter 4

Simulation Model Results

Because this model was made for the longitudinal control of the aircraft, run cases based on different velocities and rate of climbs were tested to check the responses. Before any run cases could be tested, the aircraft was first checked to make sure it responded as expected when the velocity was held constant and rate of climb kept at zero. During this check, the aircraft maintained steady level flight with differential thrust among the motors. After seeing how the aircraft responds when flying at trim conditions, the velocities and rate of climb or descent were then increased and decreased.

Increasing Velocity

The velocity was first increased from the trim velocity of 15.5 m/s to a value of 20 m/s. In Fig. 12 the velocity versus time plot shows that this occurs in a reasonable period of time with no overshoot. The controller is then able to keep the airplane flying at this new commanded velocity.

Besides making sure that the velocity increases at a reasonable rate to the required value, there are other parameters that must also be checked. The thrusts are graphed versus time to verify they are both positive and their total output is equal to the drag of the aircraft. It can be seen in Fig. 5 that once the new velocity is commanded at one second, the thrust difference between the two motors switches and motor one has a larger force, resulting in a decrease in pitch angle to allow the aircraft to stay at a constant altitude while increasing speed. This pitch

angle then goes to a steady state value of almost zero degrees as both the thrusts reach the values necessary for trim. When the model was run without changing the velocity, the steady state pitch angle was almost 3°. At this flight condition, the aircraft has no pitching moment while flying at steady level flight. The thrusts initially increase to compensate for the changes in altitude required to keep the aircraft flying at a constant height, but then go back to a steady state value to maintain the aircraft altitude as it reaches its new velocity. The steady state thrust difference is larger than when the velocity was not changed due to the relationship of velocity for calculating the thrust from the thrust coefficient. The total thrust is higher when velocity is increased due to the increase in drag caused by the higher commanded velocity. Thrust 1 is larger due to hold the decreased pitch angle from the steady state value. There is a little bit of elevator deflection for the first few seconds as the pitch angle is increasing and then decreasing, but this goes to zero as the thrust trims the aircraft.

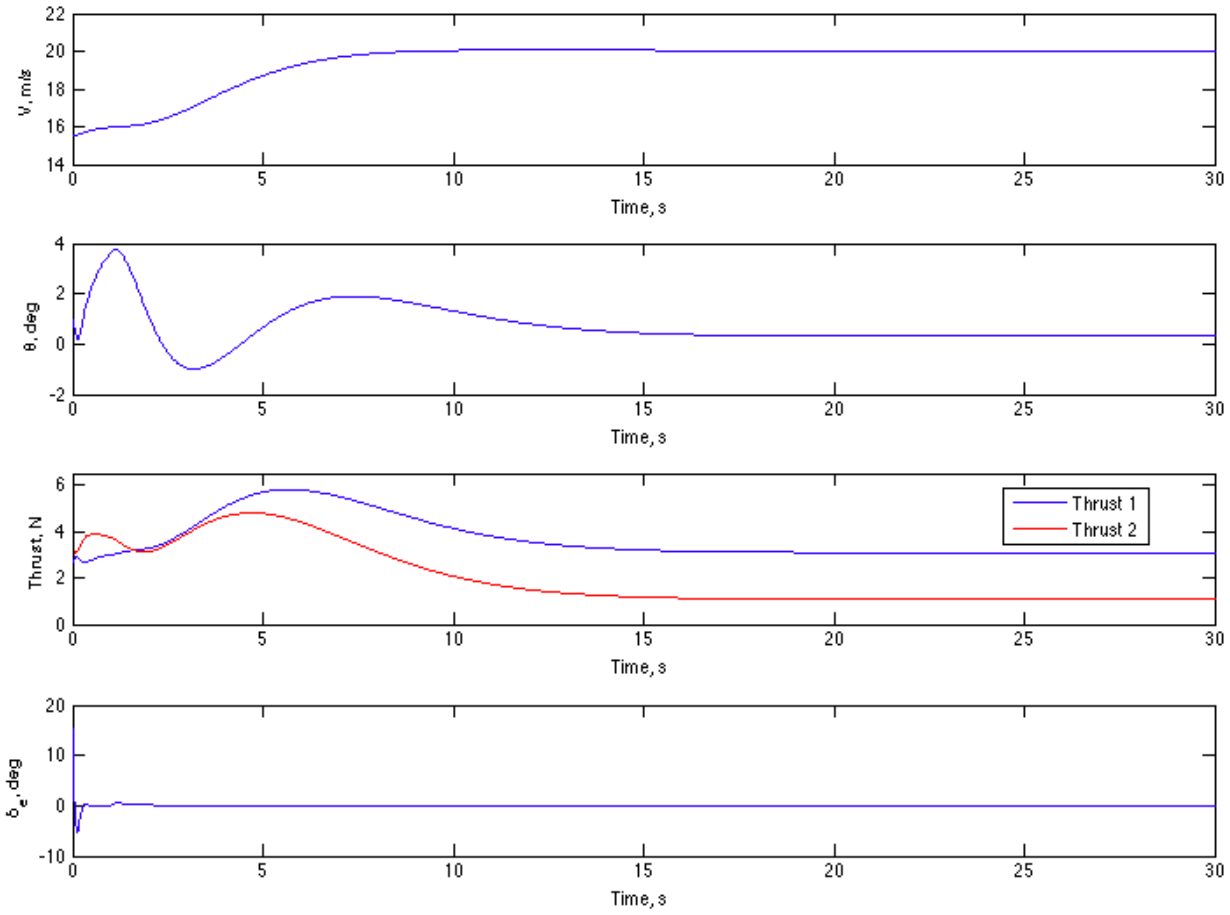

Figure 12: Aircraft Response for Increase in Velocity

Decreasing Velocity

After running the simulation for an increase in velocity, the model needed to be tested for a decrease in airspeed. The commanded velocity was decreased from the trim value of 15.5 m/s to a new value of 13 m/s, as seen in Fig. 13. Because the rate of climb is being held at zero for this case, the difference in thrust to trim the aircraft becomes greater than the total thrust required for a couple of seconds. The rate of climb initially increases when the pitch angle increases, and therefore a negative thrust is necessary to return the value to zero.

At around 4 seconds, the total thrust can be seen to go to zero before going negative. Once the negative total thrust occurs, motor 1 has a negative thrust and motor 2 has a positive

thrust. This thrust difference is necessary to maintain the pitch angle of the aircraft while descending. This is one case where flaps would be used to add drag to reduce the rate of climb. Before the total thrust goes to a value of zero, the thrust difference becomes larger than the positive total thrust, resulting in a negative thrust from motor 1. Because this negative thrust for the motor is due to a need for a large moment, and not a decrease in the forces in the positive x-direction as with negative total thrust, motor 1 is set to equal zero during this event and the elevator is deflected to aid in trimming the aircraft. From Fig. 13 it can be seen that when one thrust is zero, the other becomes a value equal to the total thrust required to maintain steady level flight. Like with the increase in velocity, the difference between the two thrust values go to a steady state value since the aircraft is not pitching for this flight condition. The difference does increase before it reaches it steady state value, however, to allow for the increase in pitch angle necessary to keep the aircraft flying at a lower velocity while maintaining its altitude. Since the pitch angle is increased for trim, motor 2 has a larger thrust than motor 1.

When the thrust value for one of the motors is set to zero, the elevator is then used to trim the aircraft to have a net moment of zero about its c.g.. In Fig. 13, the elevator is deflected not only for disturbance rejection, but is also constantly deflected at the time intervals that one or both of the thrusts are zero or negative, meaning it is actively helping to trim the aircraft.

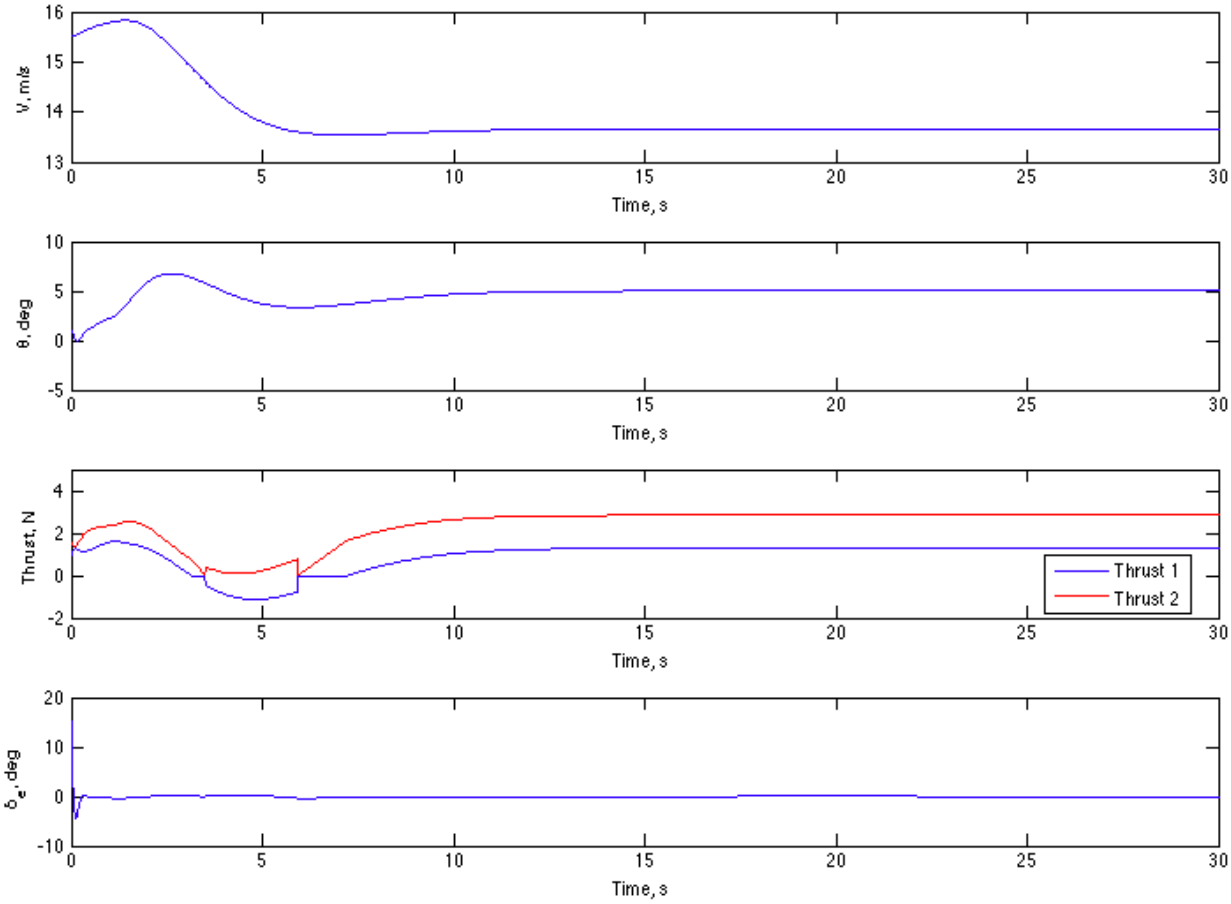

Figure 13: Aircraft Response for Decrease in Velocity

The total thrust necessary for trim flight for this case is the same as that necessary for the increase in velocity, and is greater than when flying at a greater L/D speed of 15.5 m/s. The reason for this is due to the aircraft flying at the back side of the power curve. Fig. 14 shows the power of the aircraft as a function of velocity for the flight speeds below the trim condition, and it can be seen that as the velocity decreases below 14.5 m/s, more power is necessary to fly the aircraft due to drag forces. Once the aircraft reaches its minimum speed at its maximum power, the airplane will need to decrease pitch angle to increase velocity and get back on the front side of the power curve.

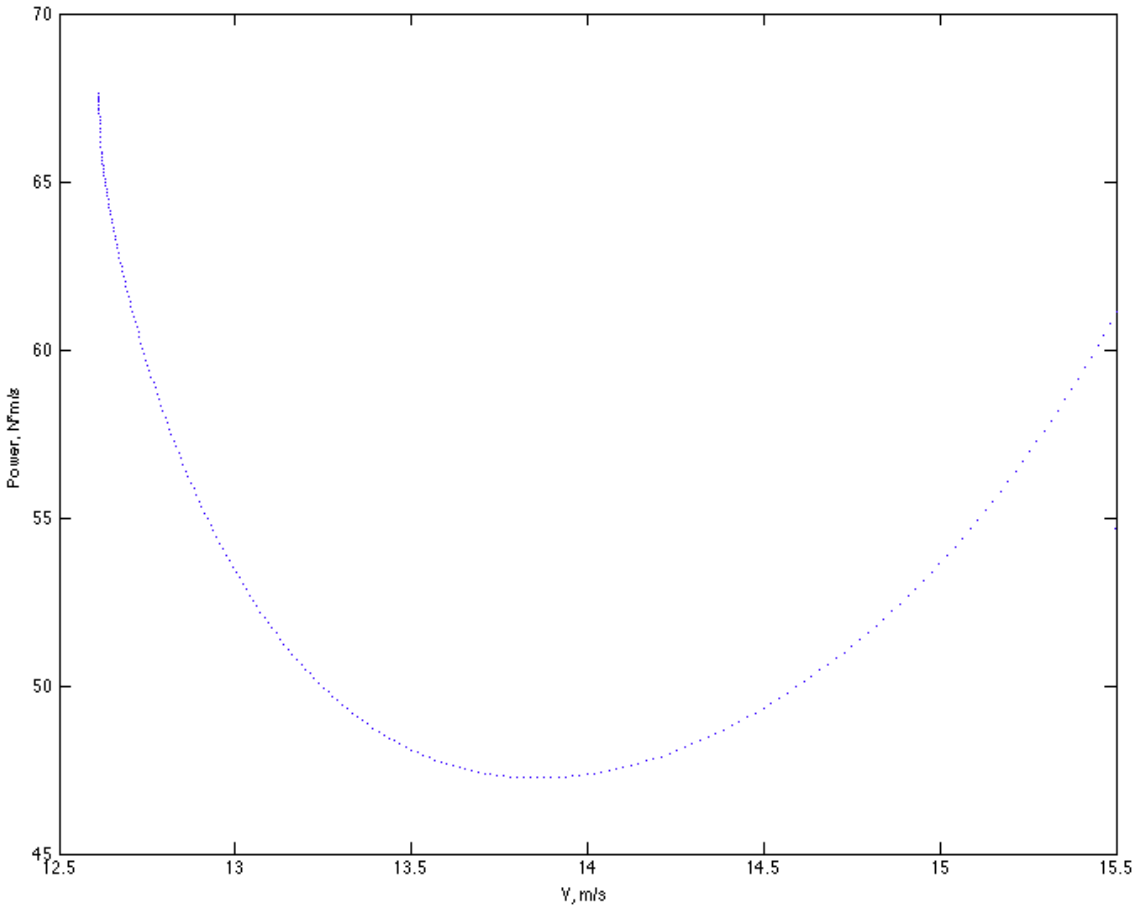

Figure 14: Power Curve for Velocities Below Trim Velocity

Positive Climb Rate

After analyzing the controller's response to different commanded velocities, the commanded rates of climb were tested. First a positive rate of climb of 1 m/s was commanded and velocity was kept constant at 15.5 m/s. The rate of climb of the aircraft is plotted in Fig. 15, and shows that initially the aircraft starts out descending, and then starts to climb at one second, when the commanded climb rate of 1 m/s occurs. In the run case where neither velocity nor rate of climb were changed, the aircraft also starts out descending and this may be due to the initialization of the elevator during the very beginning of the simulation. The increase in thrust at

a constant velocity results in a rate of climb for the aircraft since the thrust force is greater than the drag for the flight condition. Once the SB-XC reaches its commanded rate of climb, the thrusts also reach their steady state value and keep producing the necessary amount of force to maintain the climb. The difference between the two thrusts increases and then decrease as they go to a steady state value. This decrease may be a result of the aircraft flying at a lower angle of attack, 3°, than the increase in velocity case which flies at 5°. A decrease in angle of attack decreases the change in thrust difference due to the relationship in Eq .(32). The increase in pitch angle is due to the rate of climb equation,

$$\dot{h} = V sin\gamma \tag{35}$$

The flight path angle must be increased if the rate of climb is increased but velocity is held constant. Motor 2 produces a larger force than motor 1 due to the increase in pitch angle from the trim value.

While the rate of climb can be controlled by an increase in thrust, the velocity must be controlled in order to keep the aircraft climbing at a constant speed. Fig. 15 shows that the increased pitch angle of the aircraft is sufficient to keep the aircraft flying at 15.5 m/s during the climb. The velocity is slightly increased, which may be due to the aircraft trimming at a new pitch angle for the commanded climb rate. After initial elevator deflections to help the airplane trim, the elevator deflection goes to zero as the thrust difference trims the aircraft to have no moment about its c.g.

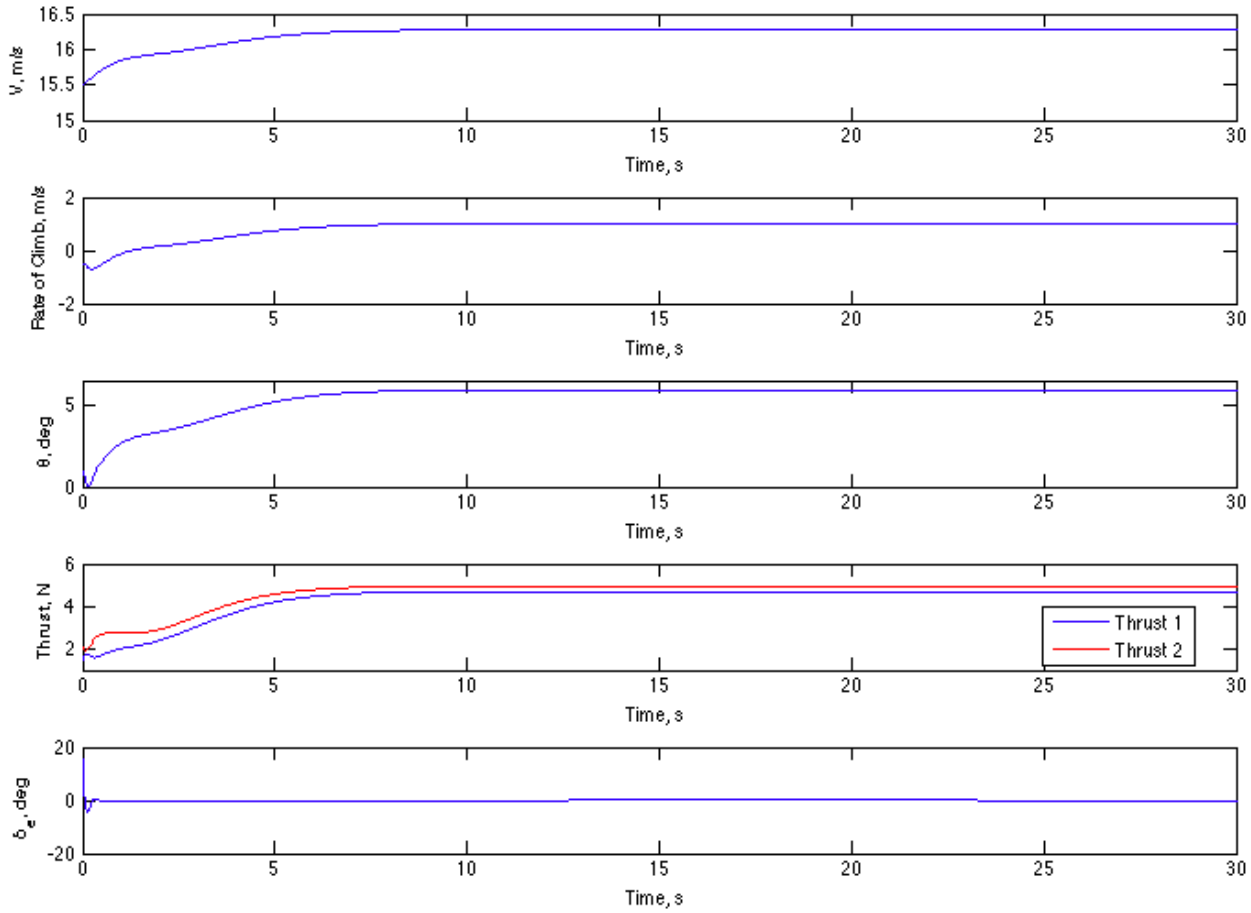

Figure 15: Aircraft Response to Commanded Climb Rate

Negative Climb Rate

The rate of climb controller must be able to control the aircraft's descent rate in addition to its climb rate. To test this case, the commanded rate of climb was -1 m/s while the velocity was again held constant at its trim value of 15.5 m/s. In Fig. 16, it can be seen that the aircraft starts at its initial descent rate of around -0.5 m/s, and then goes to a value of -1 m/s and holds that descent rate. Due to the descent rate, the total thrust needed becomes negative. Usually to decrease altitude, flaps or spoilers would be utilized to make the drag larger than the available thrust. In this case, the drag is kept fairly constant because of the constant velocity, and the total

thrust must then become negative for a negative rate of climb, due to Eq. (29). The pitch angle goes to a negative steady state value since the aircraft is descending while maintaining trim velocity. Motor two has a slightly less negative thrust than motor one due to the negative pitching moment necessary to trim the aircraft for a angle lower than the trim angle. Because the elevator must compensate for thrust difference when one thrust is set to equal zero, it deflects for a few seconds during the simulation and goes back to its trim value of zero.

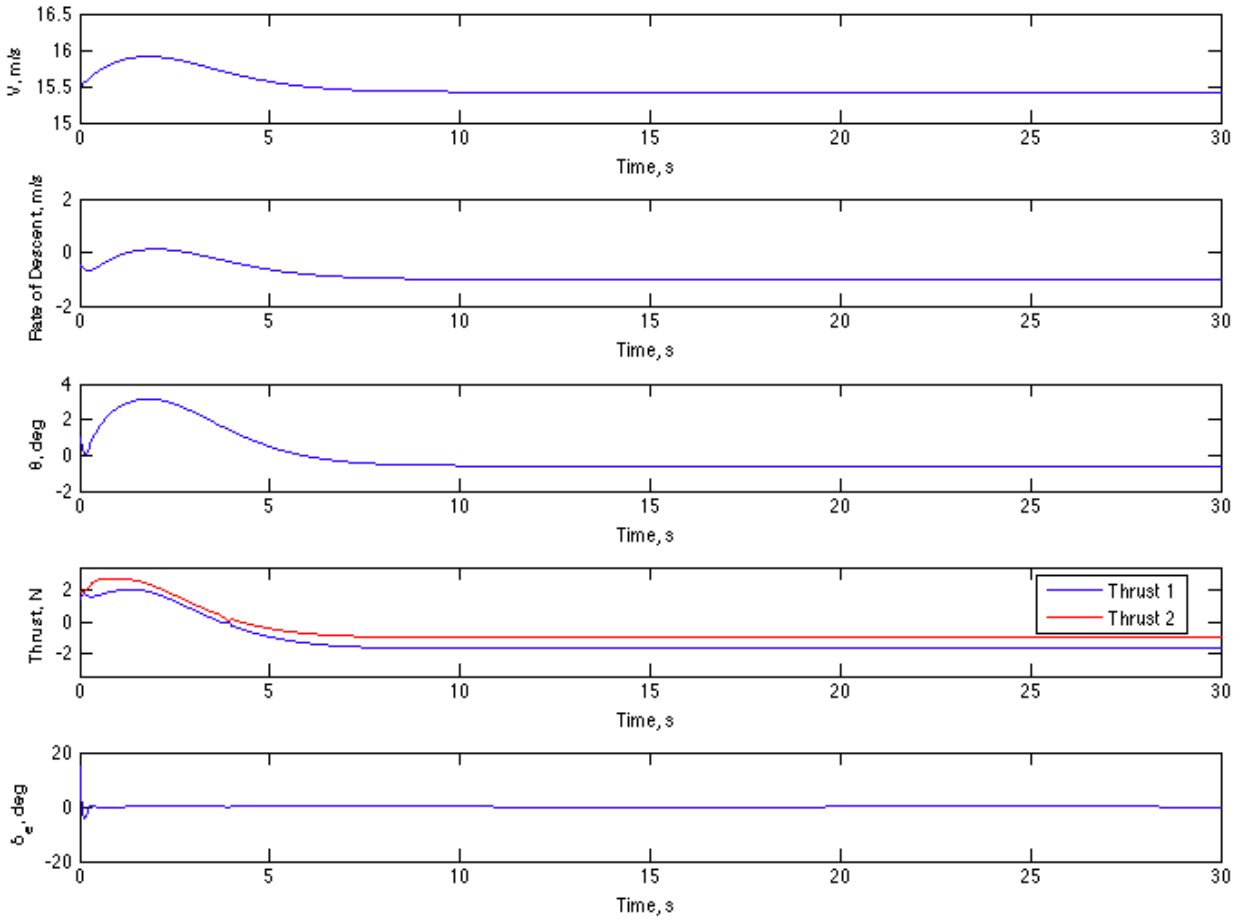

Figure 16: Aircraft Response to Commanded Descent Rate

Chapter 5

Conclusion

After running the test cases for the Simulink model, it can be determined that longitudinal control is possible via distributed propulsion and elevator deflection for disturbance rejection. Differential thrust across the motors can successfully control the rate of climb of the aircraft, and provide the necessary moments to maintain steady level flight. The elevator deflection is used only for disturbance rejection or to correct for the event of negative thrust. Flaps would be necessary to add for future analysis in order to increase drag so that the airplane is able to reduce its speed or descend without the need for negative thrust. Another idea to implement would be adding the dynamics for the motor lag into the model. This would result in more accurate responses since the motors cannot instantaneously change their thrust force. Also, since it was found that engine delay decreases with velocity, an analysis could be conducted to determine the ideal speed range for elevator use versus the speed range for differential thrust for optimal efficiency and control. Besides longitudinal control, lateral control should be added in order to analyze the use of differential thrust as opposed to rudder deflection.

Appendix A

Vehicle Properties

m	10 kg
b	4.34 m
c	0.232 m
S	1 m^2
I_{yy}	1.87 $kg.m^2$
C_{L0}	0.37
$C_{L\alpha}$	5.54 /rad
C_{LQ}	-3.255 s/rad
$C_{L\dot{\alpha}}$	-0.651 s/rad
$C_{L\delta f}$	1.63 /rad
C_D	$0.1723x^4-0.3161x^3+0.2397x^2-0.0624x+0.0194$
x	$C_{L0}+C_{L\alpha}\,\alpha$
$C_{D\delta e}$	0 /rad
$C_{D\delta f}$	0.042 /rad
C_{m0}	0.01
$C_{m\alpha}$	-0.277 /rad
C_{mQ}	-14.6 s/rad
$C_{m\delta e}$	1.6275 /rad

Appendix B

Nomenclature

c = chord

g = gravitational constant

I_{yy} = moment of inertia about y-axis

m = mass

ρ = air density

S = wing area

v = airspeed

z = motor distance in z-direction from center of gravity

C_D = drag coefficient

$C_{D\delta e}$ = ∂CD/∂δe

C_L = lift coefficient

C_{L0} = lift coefficient at α=0

$C_{L\alpha}$ = ∂CL/∂α

C_M = pitching moment coefficient

C_{M0} = pitching moment coefficient at α=0

$C_{M\alpha}$ = ∂CM/∂α

$C_{M\delta e}$ = ∂CM/∂δe

C_{Mq} = ∂CM/∂q

K_n = static margin

ζ = damping ratio

ω_n = natural frequency

θ = pitch angle

α = angle of attack

γ = flight path angle

K_i = integral gain

K_p = proportional gain

K_d = derivative gain

REFERENCES

[1]Langelaan, J., W., "Gust Energy Extraction for Mini- and Micro- Uninhabited Aerial Vehicles," *AIAA Journal of Guidance, Control, and Dynamics*, Vol. 1, No. 2, 2009, pp. 464-473.

[2]Stepanyan, V., Krishanakumar, K., and Nguyen, N., "Adaptive Control of a Transport Aircraft Using Differential Thrust", NASA, Moffett Field, California, Aug 2009.

[3]Burcham, F. W., and Bull, J., "Using Engine Thrust for Emergency Flight Control: MD-11 and B-747 Results", NASA/TM-1998-206552, NASA, Edwards, California, May 1998.

[4]Harefors, M., and Bates, D. G., "Integrated Propulsion-based Flight Control System Design for a Civil Transport Aircraft", Proceedings of IEEE, Institute of Electrical and Electronics Engineers, Sept. 2002.

[5]David, H., Michael, D., A., "No Flight Controls," *Aviation Week and Space Technology*, Vol. 159, No. 23, 8 Dec. 2001, pp. 42-43.

[6]Simulink, Software Package, Ver. 7.1, The MathWorks, Natick, MA, 2012b.

[7]Etkin, B., and Reid, L. D., Dynamics of Flight, 3rd ed., John Wiley & Sons, New Jersey, 1996.

[8]MATLAB, Software Package, Ver. 7.6.0.324, The MathWorks, Natick, MA, 2012b.

[9]Franklin, G., F., Powell, J., D., Emami-Naeini, A., Feedback Control of Dynamic Systems, 6th ed., Pearson Higher Education Inc., NJ, 2010.

[10]Sogami, H., "Lauda Air B767 Accident Report," Aircraft Accident Investigation Committee, Ministry of Transport and Communications, Thailand.

ACADEMIC VITA

Charlotte S. Gill
421 Hemlock Lane
Chester Springs, PA 19425
(610) – 806 – 2015
csgill8@gmail.com

Education:

Bachelor of Science in Aerospace Engineering
Minor in Information Sciences and Technology for Aerospace Engineers
Schreyer Honors College
The Pennsylvania State University, University Park, PA

Professional Experience:

The Boeing Company, Stress Engineer Intern - Everett, Washington 05/13-08/13
Engineering Accelerated Hiring Special Initiative

- Assisted 777 fleet support team with stress analysis on repairs using structural analysis software
- Produced repair instructions in response to telexes from airlines
- Conducted initial development of rework limits for a flap support actuator fitting with FEM software

Activities:

Flight Vehicle Design and Fabrication, 8-semester Aerospace Honors Class 01/11-Present

- Working with classmates to design and construct a human powered aircraft to win the Kremer Prize
- Conducting stability and control analysis for efficient course navigation
- Constructed composite aircraft components using carbon fiber and fiberglass
- Co-led a team to build an RC aircraft for the Design/Build/Fly competition
- Managed and delegated tasks to complete the 60 page technical report for DBF

Autonomous Underwater Vehicle Design, 2-semester Aerospace Design Class 08/13-Present

- Determining initial design requirements for a vehicle for the 2014 AUVSI RoboSub Competition
- Designing low-level control for the AUV as a part of the Modeling and Control team

Aerodynamics II Computational Fluid Dynamics Class Project 04/13-05/13

- Computed the flow field around an airfoil using CDF software
- Analyzed aerodynamic characteristics at various Mach numbers and angles of attack

Association Memberships/Honors:

Secretary, Sigma Gamma Tau (National Aerospace Engineering Honors Society) 05/13-Present

- Webmaster for Penn State Sigma Gamma Tau website

Committee Chair, Society of Women Engineers 08/10-05/12

- Assisted in organizing and planning community service events

Mentor, Schreyer Honors College Gateway Orientation for New Scholars 05/12-Present

- Working in teams to prepare orientation and provide advice to new scholars

Member, American Institute of Aeronautics and Astronautics 08/10-Present
Member, Tau Beta Pi (National Engineering Honors Society) 08/13-Present